Leucine enhances aerosol performance of Naringin dry powder and its activity on cystic fibrosis airway epithelial cells

Lucia Prota, Antonietta Santoro, Maurizio Bifulco, Rita P. Aquino, Teresa Mencherini, Paola Russo*

Department of Pharmaceutical and Biomedical Sciences, University of Salerno, Via Ponte don Melillo, 84084 Fisciano, SA, Italy

ABSTRACT

The effect of different amino acids (AAs) on the aerosol performance of N spray-dried powders was studied. Morphology, size distribution, density, dissolution rate were evaluated and correlated to process parameters. The aerosol performance was analyzed by both Single Stage Glass Impinger and Andersen Cascade Impactor. Results indicated that powders containing 5% (w/w) of leucine, proline or histidine and dried from 3:7 ethanol/water feeds showed very satisfying aerodynamic properties with fine particle fraction > 60%. Both neat N (raw and spray-dried) and N-leu1 dry-powder showing good aerodynamic properties were tested in cystic fibrosis (CF) and normal bronchial epithelial cells. Cell proliferation and expression levels of the key enzymes of the NF-κB and MAPK/ERK pathways, overactivated in CF cell lines, were evaluated. N-leu1 was able to significantly inhibit the expression levels of IKKα, IKKβ, as well as of the direct NF-κB inhibitor, IκBα. In addition N-Leu1 inhibited phosphorylation of ERK1/2 kinase and did not reduce cell proliferation as observed for the neat raw drug. Leucine co-spray-dried with the drug improved both aerodynamic properties and *in vitro* pharmacological activity of Naringin. The optimized N-Leu formulation as dry powder is potentially able to reduce hyperinflammatory status associated to CF.

© 2011 Elsevier B.V. All rights reserved.

1. Introduction

Cystic Fibrosis (CF) is the most common lethal autosomal genetic disorder, caused by mutations in the gene encoding the Cystic Fibrosis Transmembrane Conductance regulator (CFTR). CFTR is an ATP-gated chloride channel regulating epithelial surface fluid secretion, mainly in respiratory and gastrointestinal tracts (Akabas, 2000). The most common mutation, the deletion of phenylalanine 508 (ΔF508), causes a CFTR folding defect and premature degradation by the proteasome (Akabas, 2000; Lukacs et al., 1994). Loss of functional CFTR promotes depletion and increases oxidation of the airway surface liquid, tissue injury, modification of intracellular signaling pathways, cell apoptosis and inflammatory processes (Jacquot et al., 2008). CF patients show a typical phenotype characterized by persistent chronic pulmonary infections and associated airway inflammation, leading to respiratory failure. Bronchoalveolar fluid of CF newborns contains increased levels of proinflammatory cytokines and neutrophils, also in absence of bacterial or viral infection (Khan et al., 1995; Zaman et al., 2004). CF bronchial epithelial cells show over-expression of proinflammatory mediators, such as cytokines IL-6 and IL-8 (Jacquot et al., 2008; Lyczak et al., 2002). Concerning this issue, it has recently been demonstrated that the nuclear factor-κB (NF-κB) and mitogen-activated protein kinase/extracellular signal-regulated kinase (MAPK/ERK) pathways are intrinsically overactivated in various CF cell lines (Rottner et al., 2007; Verhaeghe et al., 2007).

Current CF therapy is directed to reduce the abnormal inflammation and abnormal mucus secretion, in order to delay the onset of CF lung tissue damage (Kieninger and Regamey, 2010; Ross et al., 2009). Only a few anti-inflammatory drugs are available for CF treatments (mainly oral corticosteroids and ibuprofen), while high doses of oral N-acetylcysteine, a well known glutathione prodrug, have shown the ability to counter the redox imbalance in CF (Jacquot et al., 2008). However, these drugs have limited beneficial effects in presence of considerable side effects. Among natural polyphenols, flavonoids such as Naringin (N) obtained from grapefruits showed anti-inflammatory, antioxidant and anticarcinogenic effects (Limasset et al., 1993). In addition, flavonoids may act as CFTR direct activators, stimulating transepithelial chloride transport (Azbell et al., 2010; Pyle et al., 2009; Springsteel et al., 2003;

Virgin et al., 2010; Wegrzyn et al., 2010). Recently, other polyphenols such as pyrogallol has shown anti-inflammatory properties in CF bronchial epithelial cells exposed to *Pseudomonas aeruginosa* (Nicolis et al., 2008). Inhalation products (Chuchalin et al., 2009; Heijerman et al., 2009; Parlati et al., 2009) seem to be an alternative to oral and parenteral drug administration for long-term CF treatment.

Among inhalation delivery systems, DPIs (dry powder inhalers) are versatile therapeutic systems, dispensing a metered quantity of powder in a stream of air, drawn through the device by the patient own inspiration in absence of propellants.

Several strategies (Pilcer and Amighi, 2010) including excipient systems have been suggested to improve flowability and, consequently, aerosol efficiency of dry powders. Current excipients approved for pulmonary drug delivery are limited to few sugars (lactose, mannitol and glucose) and an hydrophobic additive (magnesium stearate) (Pilcer and Amighi, 2010), due to potential toxicity for lung. As a matter of fact, safe amino acids (AAs) co-spray-dried with few active compounds showed the ability to modulate drug aerosolization behaviour (Chew et al., 2005a; Lucas et al., 1999; Najafabadi et al., 2004). To support AAs pulmonary safety, a formulation of Aztreonam and lysine (Cayston®, powder for instant solution and inhalation) has been recently approved by FDA for CF patients.

The aim of this research was to improve the aerosol performance of N-dry powder by co-spray drying different AAs (arginine, histidine, lysine, leucine, proline and threonine). Morphology and surface, size distribution, density, dissolution rate of a number of N-AAs powders were examined. Moreover, their aerodynamic properties were studied using Turbospin® as device and correlated to the feed composition (ethanol/water and AA/drug ratios) and AA nature. The optimal formulation identified in N-leu 1 (N co-sprayed with 5% leucine) was tested in increasing concentrations *vs* commercial grade N (rawN) and N in spray-dried form (N-1) on bronchial epithelial cells bearing a CFTR ΔF508/ΔF508 mutant genotype (CuFi1) and normal bronchial epithelial cells (NuLi1) (Dechecchi et al., 2008; Zabner et al., 2003). Efficacy in reducing CF intrinsic inflammation was determined as the ability to modulate the expression levels and phosphorylation status of key enzymes of the MAPK/ERK and NF-κB signaling pathways.

2. Materials and methods

2.1. Chemicals

Naringin, L-AAs (arginine, histidine, leucine, lysine, proline, threonine), dimethil sulphoxide (DMSO) and sodium hydroxide anhydrous pellets were supplied by Sigma–Aldrich (Milan, Italy). Ethanol 96% and dichloromethane (for analysis, USP grade) were purchased from Carlo Erba Reagents (Milan, Italy). Size 2 gelatine capsules were kindly offered by Qualicaps Europe S.A. (Madrid, Spain). The device used for aerodynamic tests was Turbospin® kindly donated by PH&T SpA (Milan, Italy). All the cell culture reagents were purchased from Lonza.

2.2. Powders preparation and yield

Micronized particles were prepared by co-spray drying N and the AA (total powder concentration 2%, w/v) from different hydro-alcoholic feeds. Formulation parameters were (i) kind of AA, (ii) N to excipient ratio (100:0, 95:5 and 90:10 (w/w), respectively) and (iii) ethanol/water ratio, ranging between 3:7 (v/v) to 1:1 (v/v). N was solubilized into ethanol and the selected AA into water. The solutions were neutralized with 1 N sodium hydroxide (about 200 μL) and spray-dried using a Buchi B-191 mini spray dryer (Buchi Laboratoriums-Tecnik, Switzerland).

Applied process parameters, selected on the basis of pilot experiments, were: inlet temperature 110 °C, approximate outlet temperature 68–72 °C, drying air flow 500 L/min, aspirator capacity 100%, air pressure 6 atmospheres, feed rate 5 ml/min, nozzle 0.5 mm. As a reference, powders of neat AA (0.2%, w/v) from 3:7 (v/v) ethanol/water feed were produced under the same operative conditions.

Each preparation was carried out in triplicate. All the spray-dried powders were collected and stored under vacuum for 48 h at room temperature. Production yields were expressed as weight percentage of the final product over the total amount of sprayed material (Table 1).

2.3. Powders physico-chemical properties

2.3.1. Particle size

Particle size of both raw materials and microparticles were determined using a light-scattering laser granulometer equipped with a micro-liquid module (LS 13 320 Beckman Coulter Inc., Fl, USA). The LS 13 320 uses a 5 mW laser diode with a wavelength of 750 nm and reverse Fourier optics incorporated in a fibre optic spatial filter and binocular lens systems. In preliminary studies, dichloromethane was chosen as suspending medium of choice (Sansone et al., 2009). Samples were suspended in dichloromethane and sonicated for 2 min: few drops of each sample were poured into the small-volume cell to obtain an obscuration between 8 and 12%. Particle size distributions were calculated by instrument software, using the Fraunhofer model. Results were expressed as d_{50} and span, defined as $[d(90) - d(10)]/d(50)$, where $d(10)$, $d(50)$ and $d(90)$ indicate diameters at the 10th, 50th and 90th percentiles of the particle size distribution, respectively.

2.3.2. Particle morphology

Morphology of raw materials and microparticles was examined using a scanning electron microscope (SEM) Zeiss EVO MA10 (Carl Zeiss SMT AG, München-Hallbergmoos, Germany) operating at 14 kV.

2.3.3. DSC analysis

Differential scanning calorimetry (DSC) was performed with an Indium-calibrated Mettler Toledo DSC 822e (Mettler Toledo, OH, USA). Accurately weighed samples (3–5 mg) (MTS Mettler Toledo microbalance, OH, USA) were placed in a 40 μL aluminium pan, which was sealed, pierced and exposed to two thermal cycles, as reported elsewhere (Sansone et al., 2009). In the dehydration cycle measurements, the sample was heated up to 130 °C at a heating rate of 20 °C/min and kept at 130 °C for 15 min to remove the residual solvent. Afterwards, the samples were cooled down to 25 °C and heated up to 350 °C at a heating rate of 10 °C/min.

2.3.4. X-ray diffraction studies

Dried samples were studied by means of X-ray diffraction measurement (XRD) with a Rigaku D/MAX-2000 diffractometer (Rigaku Corporation, Tokyo, J) using a Ni-filtered Cu-Kα radiation (40 kV, 20 A). 2θ range was set from 5 to 50°, step size 0.03°/2θ and 5 s counting time per step. A Rigaku imaging plate, mod. R-AXIX DSBC, was used for digitizing the diffraction patterns.

2.3.5. Bulk and tapped density

The bulk and tapped density of the spray-dried powders were measured as described elsewhere (Sansone et al., 2009). Briefly, powders were loaded into a bottom-sealed 1 mL plastic syringe (Terumo Europe, Leuven, Belgium) capped with laboratory film (Parafilm® "M", Pechiney Plastic Packaging, Chicago, IL, USA) and tapped on a hard bench until no change in the volume of the powder was observed. The bulk density was calculated from the difference

Table 1
Formulation parameters and responses of N and N/AA dry powders.

Code #	% AA[a]	Feed solution[b]	Spray yield (%)	d_{50} (μm) (Span)	Code #	% AA[a]	Feed solution[b]	Spray yield (%)	d_{50} (μm) (Span)
N-1	–	3:7	59.4	5.20 (1.56)	N-pro 3	5	4:6	60.6	2.93 (2.05)
N-2	–	4:6	61.2	4.10 (1.68)	N-pro 4	10	4:6	67.8	2.99 (2.08)
N-3	–	1:1	55.9	6.99 (1.71)	N-pro 5	5	1:1	66.7	2.74 (1.77)
N-leu 1	5	3:7	60.7	3.31 (1.68)	N-pro 6	10	1:1	64.7	5.34 (1.93)
N-leu 2	10	3:7	54.4	2.88 (1.47)	N-his 1	5	3:7	51.3	2.99 (1.80)
N-leu 3	5	4:6	68.5	3.02 (1.70)	N-his 2	10	3:7	50.6	2.00 (1.85)
N-leu 4	10	4:6	60.6	2.82 (1.44)	N-his 3	5	4:6	62.6	4.21 (1.83)
N-leu 5	5	1:1	69.0	2.80 (1.74)	N-his 4	10	4:6	64.1	4.12 (1.92)
N-leu 6	10	1:1	63.2	2.75 (1.64)	N-his 5	5	1:1	72.0	4.44 (1.72)
N-pro 1	5	3:7	69.0	2.78 (1.73)	N-his 6	10	1:1	71.5	3.72 (1.77)
N-pro 2	10	3:7	60.0	3.42 (1.82)					

[a] Relative amount of AA by % in weight compared to the total amount of dry substance (2%, w/v).
[b] EtOH/water (v/v) content in the feed.

between the weight of the plastic syringe before and after loading divided by the volume of powder in the syringe. The tapped density was calculated from the difference between the weight of the plastic syringe before and after loading divided by the volume of the powder in the syringe after tapping. Experiments were performed in triplicate.

2.4. Aerodynamic behaviour evaluation

The *in vitro* deposition of the micronized powders was evaluated using a single-stage glass impinger (SSGI, apparatus A European Pharmacopoeia 6.0, Copley Scientific Ltd., Nottingham, UK). A water/ethanol 8:2 (v/v) mixture was introduced in the upper (7 mL) and lower (30 mL) stages of the SSGI. Hard gelatine capsules (size 2) were filled manually with 20.0 ± 0.5 mg of spray-dried powders. Then, the capsule was introduced into the Turbospin® and pierced twice. The vacuum pump was operated at a flow rate of 60 L/min for 5 s (Erweka vacuum pump VP 1000 equipped with an electronic digital flowmeter type DFM, Erweka Italia, Seveso (MI), Italy). Each deposition experiment was performed on 10 capsules and repeated in triplicate. Upper and lower stages were washed with 500 ml of an 8:2 (v/v) water/ethanol mixture.

The N deposited into the upper and lower stages of the impinger was evaluated by UV detection (UV/vis spectrometer Lambda 25, Perkin Elmer instruments, MA, USA) at a wavelength of 283 nm, using 1 mm spectroscopy SUPRASIL® quartz cell (100-QS, Hellma Italia srl, Milan, I). Calibration curves were previously worked out and proportionality between N concentration and absorption was verified in the range of 70–400 mg/L. The emitted dose (ED) was gravimetrically determined and expressed as percentage of powder exiting the device *vs* amount of powder introduced into the capsule (Giry et al., 2006). The fine particle fraction (FPF), defined as ratio of N recovered from the lower stage of SSGI *vs* total N charged into the capsules, was expressed as a percentage (Sansone et al., 2009).

The powders showing promising aerosolisation properties were also tested with an Andersen cascade impactor (apparatus D, European Pharmacopoeia 6.0, ACI, Westech Instrument Services Ltd., Bedfordshire, UK), modified for use at a flow rate of 60 L/min as described elsewhere (Gilani et al., 2005; Seville et al., 2007). The effective cut-off diameters of the modified ACI, provided by the producer, were: Stage −1, 8.6 μm; Stage −0, 6.5 μm; Stage 1, 4.4 μm; Stage 2, 3.2 μm; Stage 3, 2.0 μm; Stage 4, 1.1 μm; Stage 5, 0.54 μm; Stage 6, 0.25 μm. To minimize particle bounce, metal impaction plates were dipped into an *n*-hexane solution of SPAN 80 (0.1%, w/v) and the solvent was allowed to evaporate, leaving a thin film of SPAN 80 on the plate surface. The ACI was assembled placing a filter paper on the filter and the Turbospin® was fitted into a rubber mouth piece attached to the throat. The vacuum pump was actuated for 4 s. The powder deposited into the different stages was recovered by plunging each plate and the stage below

into a water/ethanol mixture 8:2 (v/v) (5–200 mL depending on the stage number). N content was assessed by UV measurements and the emitted dose (ED) was determined as described above for SSGI experiments. The cumulative mass of powder with a diameter lower than the stated size of each stage was calculated and plotted as a percentage of recovered powder *vs* cut-off diameter. The mass median aerodynamic diameter (MMAD) of the particles was extrapolated from the graph, according to the European Pharmacopoeia 6.0. From the same plot, the fine particle dose (FPD), i.e. the mass of N with a particle size less than 5 μm, and the fine particle fraction (FPF), i.e. the fraction of N emitted from the device with a particle size less than 5 μm, were determined (European Pharmacopoeia 6.0).

In vitro deposition experiments were performed on three batches with three replicates each.

2.5. Dissolution study

Information about immediate solubility of the powders was obtained by a modified dissolution test (Hancock and Parks, 2000). Briefly, an excess of micronized powder (1.6 g) was introduced together with a magnetic bar into a 40 mL closed, flat-bottomed glass vial, and 25 mL of distilled water heated at 37 °C were added. The dissolution medium was kept at 37 °C in a water bath under magnetic stirring at 300 rpm: at regular time intervals the liquid phase was withdrawn, replaced with distilled water at the same temperature, filtered with 0.45 μm filters, diluted and analyzed by UV–visible spectroscopy for N content. Dissolution tests were carried out in triplicate and monitored for 120 min. Results obtained after 30 min are reported.

2.6. Biological activity

2.6.1. Cell lines and culture conditions

CuFi1 and NuLi1 cell lines, derived from human bronchial epithelium of a CF (CuFi1, CFTR ΔF508/ΔF508 mutant genotype) and a non-CF subject respectively (NuLi1, WT CFTR), (Zabner et al., 2003) were purchased from American Type Culture Collection (ATCC, Manassas, VA, USA). CuFi1 and NuLi1 cells were grown in human placental collagen type VI coated flasks (Sigma–Aldrich, Milan, Italy) in BEGM medium (Lonza Walkersville. Inc). Cells were incubated at 37 °C in a humidified atmosphere containing 5% CO_2.

2.6.2. Proliferation assay

Cell growth was assessed by using a colorimetric bromodeoxyuridine (BrdU) cell proliferation ELISA kit (Roche Diagnostics, Milan, Italy). Briefly, 5×10^3 cells were seeded into each coated well of a 96-well plate and left to adhere to the plate. The cells were then treated with increasing concentrations (from 15 to 150 μM) of rawN, N-1 and N-leu 1 for 24 h, and BrdU was added for the final
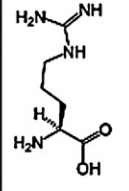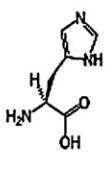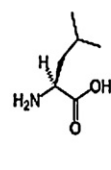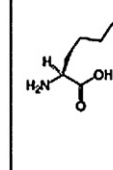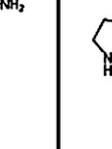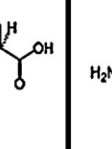
aa	Arginine	Histidine	Leucine	Lysine	Proline	Threonine
IP	10.76	7.60	6.01	9.60	6.30	5.60
Water solubility (g/L)	148.7	38.2	24	300	1500	200

Fig. 1. Isoelectric point (IP) and water solubility of AAs selected as pulmonary excipients.

16 h (10-5 mol/L). At the end of the whole cell culture period, the medium was removed and the ELISA BrdU immunoassay was performed as described by the manufacturer. The colorimetric reaction was stopped by adding H_2SO_4, and the absorbance at 450 nm was measured using a microplate reader (Bio-Rad Laboratories, Milan, Italy).

DMSO alone (0.1% final concentration in cell culture medium) did not give any significant result in all biological *in vitro* assays.

2.6.3. Western blot analysis

For *in vitro* biological studies, the powders were dissolved in the cell culture medium and immediately administered to the cells at a concentration of 30 μM.

CuFi1 and NuLi1 cells, treated with rawN, N-1 and N-leu 1 were collected by centrifugation, washed twice with PBS and resuspended in RIPA buffer (NaCl 150 mM, 1% triton X-100 pH 8.0, 0.5% sodium deoxycholate, 0.1% SDS, 50 mM Tris, pH 8.0) at 4 °C and centrifugated at 13,000 rpm for 30 min. Supernatants were collected and protein concentrations determined by Bio-Rad protein assay. Equal amounts of protein extracts (30 μg) were boiled in Laemmli's buffer, fractioned on 12% SDS-PAGE and then transferred to nitrocellulose membranes (Amersham GE Healthcare, Milan, Italy). Membranes were blocked in TBS-T (50 mM Tris, 135 mM NaCl, and 5 mM KCl, 0,1% Tween-20) containing 5% fat free dry milk, washed in TBS-T, then incubated overnight at 4 °C with anti-IKKα, anti-IKKβ, phosphoERK1/2 (Thr202/Tyr204) and anti-phospho-IkBα (Ser32) (all from Cell Signaling Technology Inc). After three washes, blots were probed with mouse or rabbit horseradish peroxidase-conjugated secondary antibodies (Cell Signaling Technology) for 1 h at room temperature and then developed using the ECL chemiluminescence system (Amersham GE Healthcare). Finally, membranes were stripped and re-probed with total anti-ERK1/2, total anti-IkBα (Cell Signaling Technology) and anti-actin used as loading control (Abcam, Cambridge, UK). Results are the mean of at least three independent experiments with three replicates each and immunoreactive bands were quantified using Quantity One I-D analysis software (Bio-Rad).

2.7. Statistical analysis

Measurements were performed in triplicate, unless otherwise stated. Values were expressed as means of at least three experiments with three replicates each ± SD. Statistical differences between the treatments and the control were evaluated by the Student's *t*-test A (*P* values less than 0.05 were considered statistically significant).

3. Results and discussion

Manufacture of powders for inhalation with aerodynamic diameter in the range of 0.5–5 μm is a technical challenge because it requires production of particles reduced in size and respirable, while, as well known, small particles undergo strong cohesive forces, resulting in increased adhesion and poor flowability. A way to improve flow properties of micronized powders is through the addition of excipients, but those currently approved (mainly sugars) for pulmonary administration are very limited in number (Pilcer and Amighi, 2010). Thus, there is a special need for the development and test of other excipients for DPI products able to increase drug deposition in the lung, acting on the powder flow, particle size, geometry and/or surface properties. In a previous study (Sansone et al., 2009) we reported that the spray-drying process of N as commercial crystalline raw material is able to produce amorphous material, showing improved aerodynamic properties but not satisfying pulmonary deposition profiles, probably due to the particles tendency to form aggregates.

Here, various AAs possessing safety profiles for use in human pharmaceuticals (arginine, lysine, threonine, leucine, histidine and proline, Fig. 1) were co-sprayed with N with the aim to enhance the dispersibility and, consequently, the respirability of the powders.

3.1. Dry powders production and characterization

Co-spray-drying process of N with arginine, lysine (positively charged side chains) or threonine (polar neutral side chain), which display an isoelectric point (IP) far from the neutral pH of the feed solutions (Fig. 1), were performed in first place: the obtained powders were not respirable and characterized by high particle size ($d_{50} > 5$ μm) and high cohesiveness, resulting in low yield of the spray-drying process (<40%). Unsatisfying pulmonary distribution profiles upon activation of the device were also obtained (data not shown).

Using leucine, histidine and proline (AAs with an IP next to 7), very interesting results were obtained in terms of flowability and aerodynamic performance determined by both SSGI and ACI.

The powders were characterized in terms of particle size, morphology, bulk and tapped density, thermal properties and immediate solubility.
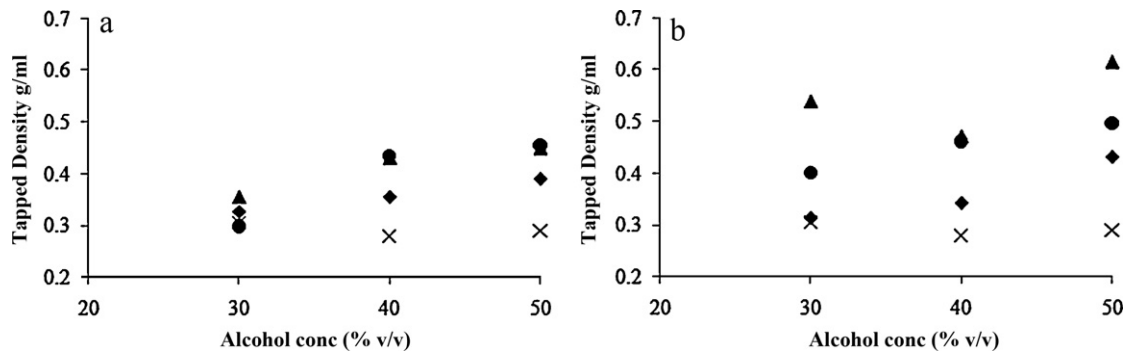
Fig. 2. Tapped density *vs* alcohol content in the liquid feed of rawN (X) and N-AA: (▲) leucine; (♦) proline, (●) histidine; (a) 5% (w/w) AA; (b) 10% (w/w) AA.

The presence of the AA in the feed formulation influenced the particle size distribution (Table 1) as well as the powder density and morphology, although the extent of these variations depends on the considered AA. The majority of the N-leu and N-pro powders showed a d_{50} within a range of 2.75–3.42 μm, very lower than powders manufactured without AAs (d_{50} 4.10–6.99 μm); only N-pro 6 has a diameter slightly above 5 μm. Increase in the ethanol ratio in the feed from 3:7 to 1:1 generally resulted in a higher process yield, ranging from about 50–60 up to 70%. Interestingly, for N-his the higher was the ethanol content, the larger were both the diameter and process yield (Table 1).

As showed by thermograms of N-leu 1 (Fig. 3c) reported as an example, DSC analyses indicated that N-AA powders produced by spray drying were amorphous materials. Spray-drying process causes the loss of crystalline habitus of both N-raw and Leu-raw as evidenced by the absence of the endotherms corresponding to N crystal melting point at 247 °C in thermogram 3b and Leu crystal melting point at 275 °C in thermogram 3a.

DSC results were confirmed by X-ray assessments, showing no crystallinity in N-AA powders produced by spray drying. As an example, X-ray patterns of crystalline N (Fig. 4a) and Leu (Fig. 4b) as raw materials were reported in comparison with X-ray pattern of N-leu 1 (Fig. 4c).

It is evident from Fig. 2 that powders containing AA possessed higher tapped density than those formulated without excipient. The density increased with the increase of both alcohol and AA content in the processed feeds. N-10% AA (Fig. 2b) feeds showed the highest tapped density values and are expected to have the worst aerosolization properties.

Microscopy observation revealed that the particles morphology was once again affected by the nature and percentage of AA as well as by ethanol content in the feed. Samples spray-dried from 3:7 ethanol/water feed and without AA, appeared as small parti-
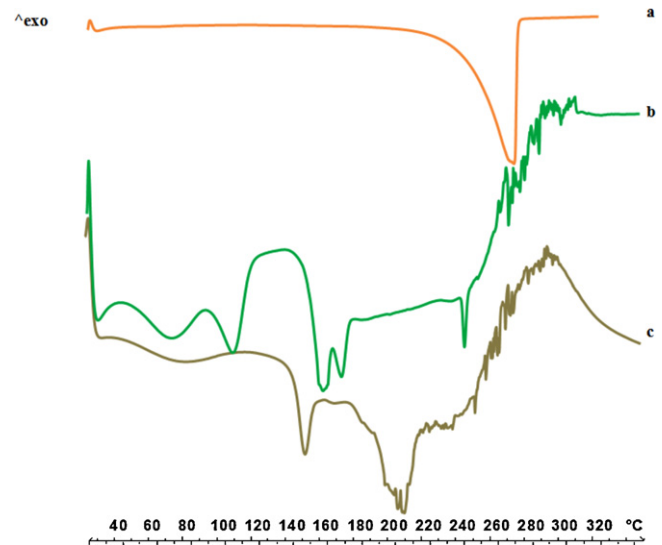

Fig. 3. Differential scanning calorimetry thermograms of leucine raw material (a), Naringin raw material (b) and N-leu 1 (c).

cles, spherical in shape or very slightly corrugated, and their SEM micrographs showed widespread aggregation (Fig. 5a). On the contrary, micrographs of samples produced with 5% AA displayed well separated particles with corrugated, raisin-like surfaces (Fig. 5b), beneficial for particles intended for inhalation. In fact, previous reports suggested that improvement of the respirable fraction may be obtained not only by lowering the aerodynamic diameter, but also reducing interparticulate cohesion (Chew and Chan, 2001; Chew et al., 2005b). Corrugated particles might also be more appro-
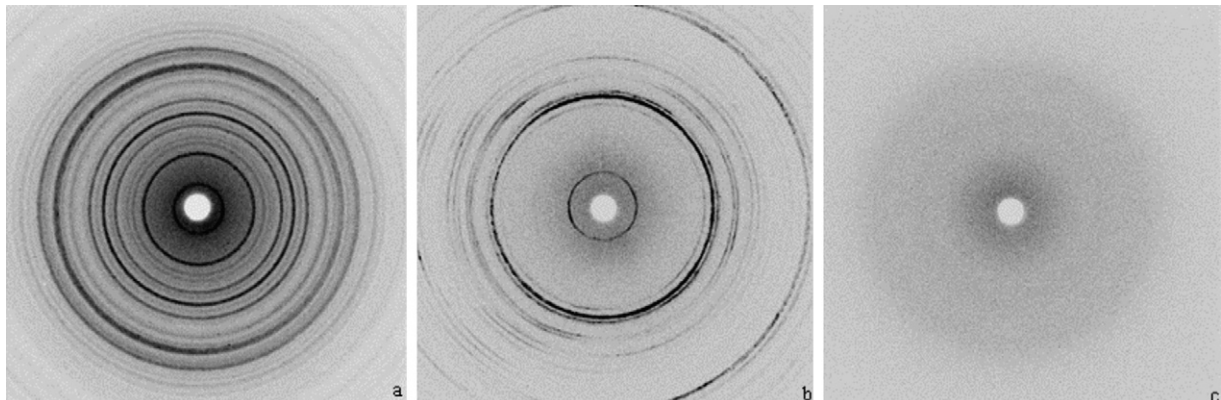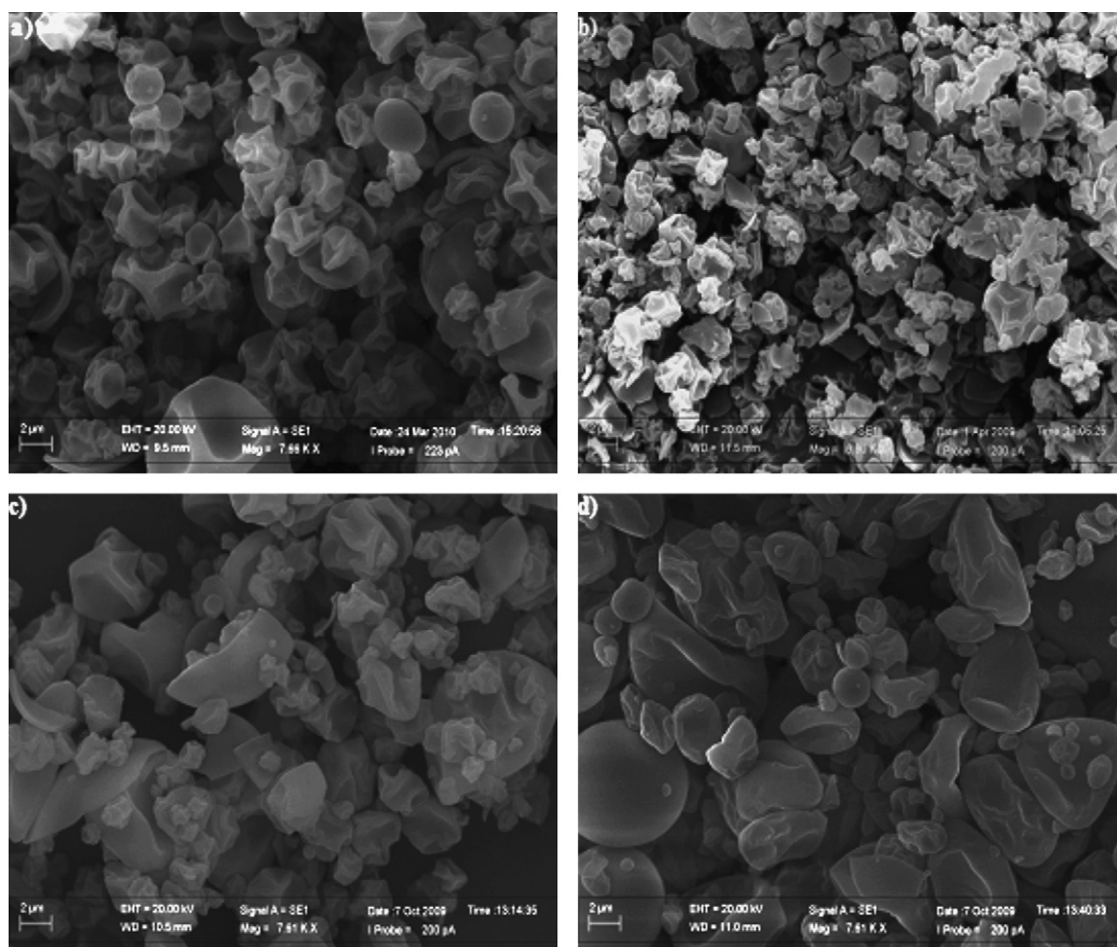

Fig. 4. X-ray patterns of Naringin raw material (a), leucine raw material (b) and N-leu 1 (c).

Fig. 5. SEM picture of (a) N–1 (ethanol/water ratio 3:7 N 2%, w/v) and N–5% histidine; (b) N–his 1 (ethanol/water ratio 3:7); (c) N–his 3 (ethanol/water ratio 4:6); (d) N–his 5 (ethanol/water ratio 1:1).

priate for dissolution in the lung fluid due to a larger surface area. When the ethanol/water ratio increased (from 3:7 to 1:1), particles with smoother surface were observed (Fig. 5c and d). Considering that increasing the ethanol content in the feed results in higher solubility of N but lower solubility of the AA, we speculate that AA may precipitate from feeds on the particle surface, shaping smoother particles (Fig. 5d, N–his). As it is well known, the spray-drying process consists of spraying a liquid solution (in this case N/AA in ethanol/water) through a nozzle to obtain liquid droplets, which are dried by solvent evaporation to form microparticles. As previously reported (Sansone et al., 2009), N has higher solubility in less polar solvents than in water (e.g. 0.11 g/100 g in water *vs* 1.1 g/100 g in ethanol), while the solubility of AAs in water is higher than in alcohols (e.g. histidine 4.30 g/100 g in water *vs* 0.76 g/100 g in water/ethanol 1/1, v/v) (Nozaki and Tanford, 1971; Peijun et al., 2009). N and AA, both soluble in a water/ethanol 7:3 mixture, are homogenously distributed in the liquid droplets and, consequently, homogenously distributed in the dry particles obtained after evaporation at 110 °C whereas AA slight soluble in water/ethanol 1:1 mixture may precipitate during the evaporation process of the droplets.

As a consequence, a larger quantity of AA deposited on the particle surface might also influence the N dissolution rate from the microparticles, modulating both wettability and interaction with the aqueous dissolution fluid. With this in mind, the immediate solubility of the batches was evaluated.

Dissolution profiles of N–5% his powders, dried from 30, 40 or 50% (v/v) ethanol feeds, are reported as an example in Fig. 6. An

evident improvement of the immediate solubility was obtained for all N–AA powders with respect to rawN. In particular, we observed the maximum enhancement in powder immediate solubility for batches N–his 5 (Fig. 6) and N–leu 5 (data not shown) prepared from feeds with the highest ethanol content (1:1 (v/v) ethanol/water) and showing the highest AA accumulation on the particle shell due to the drying process.

In addition, as previously reported for rawN spray-dried powders (Sansone et al., 2009), also N–AA microparticles rapidly decrease their solubility in few minutes of exposure to solvent, reaching a nearly constant value after 30 min (Fig. 6). Simi-
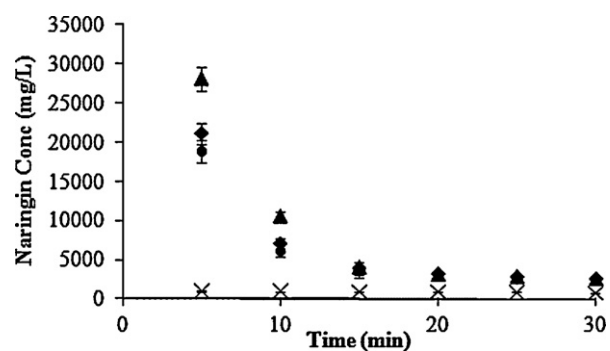
Fig. 6. Aqueous solubility at 37 °C of rawN (X) and N–5% histidine; (♦) N–his 1 (ethanol/water ratio 3:7; (●) N–his 3 (ethanol/water ratio 4:6); (▲) N–his 5 (ethanol/water ratio 1:1).

Table 2
Aerodynamic properties of N and N-AA dry powders after single stage glass impinger deposition experiments. All data are shown as mean ± SD of three experiments.

Code #	ED (%)	FPF (%)	Code #	ED (%)	FPF (%)
N-1	92.7 ± 0.0	44.5 ± 1.5	N-pro 3	88.0 ± 9.7	43.3 ± 1.7
N-2	84.2 ± 6.5	40.9 ± 1.4	N-pro 4	86.6 ± 7.2	46.1 ± 1.3[**]
N-3	83.9 ± 2.4	38.5 ± 0.1	N-pro 5	85.7 ± 2.6	38.2 ± 3.9
N-leu 1	89.5 ± 4.8	51.3 ± 1.6[**]	N-pro 6	87.4 ± 3.5	34.1 ± 2.1[*]
N-leu 2	73.6 ± 7.5	40.2 ± 1.5[*]	N-his 1	91.8 ± 4.7	49.2 ± 1.1[*]
N-leu 3	89.0 ± 5.5	52.0 ± 1.1[**]	N-his 2	85.9 ± 8.3	47.1 ± 2.0
N-leu 4	83.3 ± 4.9	50.9 ± 3.9[*]	N-his 3	92.5 ± 3.0	41.5 ± 3.1
N-leu 5	81.6 ± 7.4	45.3 ± 1.1[**]	N-his 4	88.8 ± 1.2	34.4 ± 0.8[**]
N-leu 6	81.9 ± 7.4	44.0 ± 2.9[*]	N-his 5	86.5 ± 6.5	29.7 ± 1.6[**]
N-pro 1	92.1 ± 4.7	57.2 ± 1.4[**]	N-his 6	84.0 ± 5.0	37.3 ± 1.9
N-pro 2	92.0 ± 3.7	45.6 ± 2.9			

ED, emitted dose; FPF, fine particle fraction.

[*] $P < 0.05$ *vs* control.

[**] $P < 0.01$ *vs* control.

lar profiles were observed for all the batches produced (data not shown). This behaviour may be due to a rapid conversion of the amorphous spray-dried material to a crystalline status which is characterized by lower solubility (Hancock and Parks, 2000).

3.2. Aerodynamic behaviour

The *in vitro* aerosol deposition data are reported in Tables 2 and 3. The AAs generally improved the aerodynamic

behaviour, in terms of fine particle fraction (FPF), with respect to rawN spray-dried powders (N-1, N-2, and N-3), used as controls.

In SSGI experiments (Table 2), the mass of powder delivered from Turbospin® (emitted dose, ED) was from 81.6 to 92.5%, with the exception of N-leu 2 (73%). The last result indicates that more than 27% of powder was retained in the capsule and/or in the inhaler device. The reason for such lower emission (73%) may be found in the poor flow properties of the powder. Moreover, high cohesiveness of N-leu 2 was confirmed by low process yield (54.4%) and high tapped density.
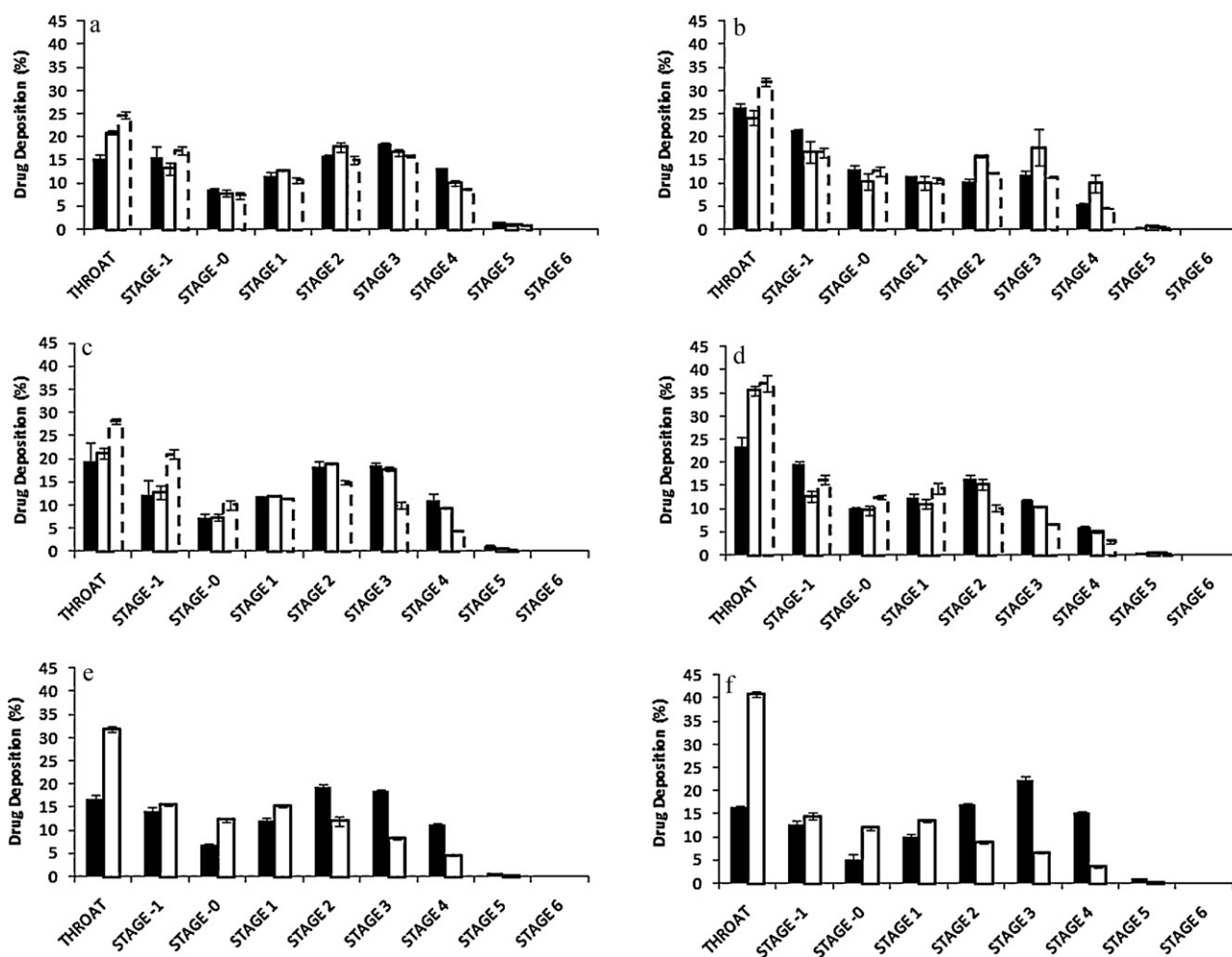
Fig. 7. Andersen cascade impactor deposition pattern of N dry powders from feeds containing: 30% (v/v) ethanol (black bars); 40% (v/v) ethanol (white bars); 50% (v/v) ethanol (dotted lines bars) and (a) 5% leucine, (b) 10% leucine, (c) 5% proline (w/w), (d) 10% proline, (e) 5% histidine, (f) 10% histidine.

Table 3
Aerodynamic properties of N and N-AA dry powders after Andersen cascade impactor deposition experiments All data are shown as mean ± SD of three experiments.

Code #	MMAD	FPF (%)	FPD (mg)	Code #	MMAD	FPF (%)	FPD (mg)
N-1	3.72 ± 0.04	44.7 ± 1.5	7.54 ± 0.8	N-pro 3	2.81 ± 0.0[**]	60.7 ± 1.2[**]	8.53 ± 0.2[*]
N-2	3.85 ± 0.06	46.0 ± 0.9	6.87 ± 0.7	N-pro 4	3.42 ± 0.1[**]	44.8 ± 1.7	6.24 ± 0.1
N-3	3.89 ± 0.15	43.0 ± 0.5	6.56 ± 0.1	N-pro 5	3.92 ± 0.1	43.9 ± 0.6	6.52 ± 0.1
N-leu 1	2.77 ± 0.06[**]	63.4 ± 1.2[**]	8.47 ± 0.1	N-pro 6	3.90 ± 0.1	42.5 ± 0.9	5.30 ± 0.2[**]
N-leu 2	4.14 ± 0.21[**]	43.2 ± 2.1	5.93 ± 0.1	N-his 1	2.75 ± 0.0[**]	64.0 ± 0.2[**]	8.87 ± 0.6
N-leu 3	2.89 ± 0.16[**]	60.7 ± 1.9[**]	8.17 ± 0.0[*]	N-his 2	2.24 ± 0.1[**]	67.4 ± 1.2[**]	7.73 ± 0.3
N-leu 4	3.13 ± 0.15[**]	54.3 ± 3.2[*]	6.39 ± 0.1	N-his 3	3.94 ± 0.1	43.9 ± 0.9[*]	6.45 ± 0.5
N-leu 5	3.06 ± 0.31[*]	53.2 ± 1.9[**]	6.61 ± 0.1	N-his 4	4.13 ± 0.1[**]	35.9 ± 1.6[**]	4.57 ± 0.7
N-leu 6	3.91 ± 0.18	42.5 ± 0.7	5.30 ± 0.1[**]	N-his 5	n.d.	n.d.	n.d.
N-pro 1	2.68 ± 0.10[**]	63.4 ± 0.5[**]	9.55 ± 0.6[*]	N-his 6	n.d.	n.d.	n.d.
N-pro 2	3.61 ± 0,11	49.7 ± 0.9[**]	6.18 ± 0.3[*]				

MMAD, mass median aerodynamic diameter; FPF, fine particle fraction; FPD, fine particle dose.
[*] $P < 0.05$ vs control.
[**] $P < 0.01$ vs control.

Table 4
Bulk density and aerodynamic properties after Andersen cascade impactor deposition experiments of selected N dry powders.

Code #	Bulk density (g/cm³)	FPF (%)	FPD (mg)
N-1	0.068	44.7 ± 1.5	7.54 ± 0.8
N-2	0.059	46.0 ± 0.9	6.87 ± 0.7
N-his 2 (20 mg)	0.094	67.4 ± 1.2	7.73 ± 0.3
N-leu 3 (20 mg)	0.095	60.7 ± 1.9	8.17 ± 0.0
N-his 2 bis (40 mg)	0.094	59.7 ± 1.2	16.2 ± 0.3
N-leu 3 bis (40 mg)	0.095	60.0 ± 2.6	18.6 ± 0.4

FPF, fine particle fraction; FPD, fine particle dose.

Despite the overall satisfying values of ED, a variation in FPF was observed depending on the AA used, its concentration and alcohol content in the feed. The highest FPFs (about 50%) were obtained for batches processed from 3:7 ethanol/water and 5% AA solutions. Generally, an increase in ethanol content (up to 40 or 50%, v/v) and AA (from 5 to 10%, w/w) concentration led to significantly lower

FPFs (from 50% to 29.7%), indicating a worsening in the powders aerosolization properties.

MMAD, FPF and FPD values derived by ACI deposition studies confirmed the observed AA and alcohol concentration-dependent trends (Table 3). For inhalation into the lower airways and into the deep lung, a better dispersibility of particles with MMAD < 5 μm is
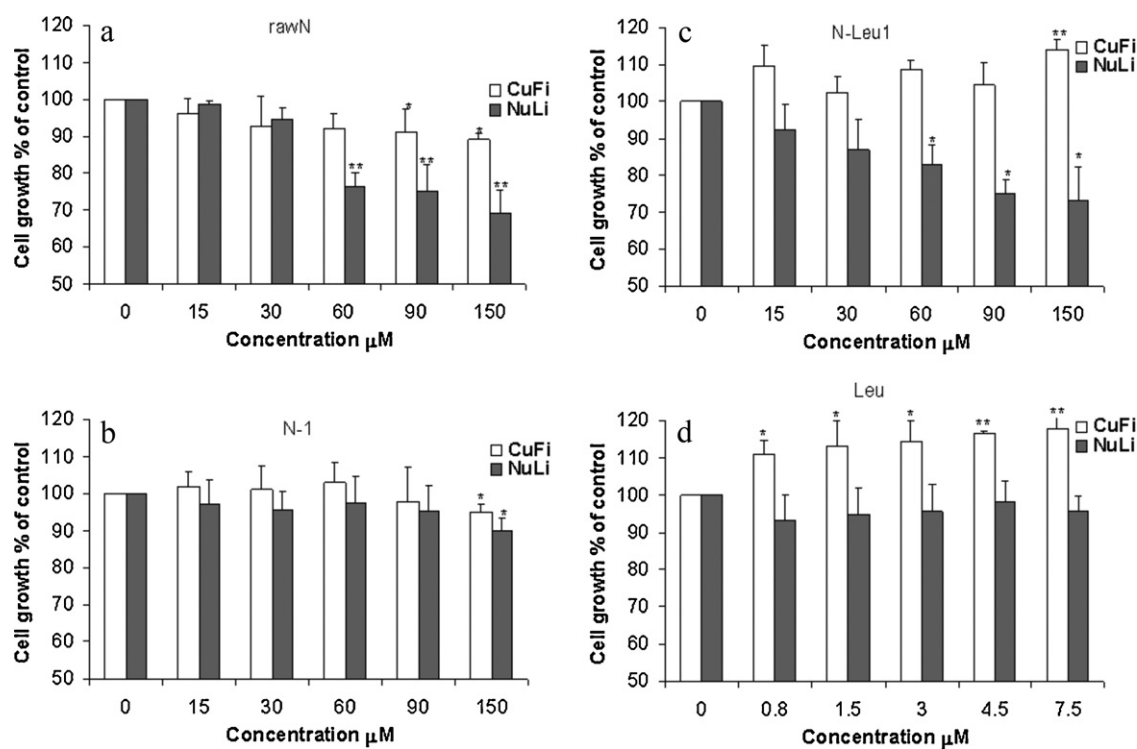
Fig. 8. Naringin and its DPI formulations do not inhibit CuFi1 and NuLi1 cell proliferation at concentrations lower than 60 μM. Cells were treated for 24 h with: (a) raw Naringin (rawN), (b) spray-dried Naringin (N-1), (c) N co-sprayed with 5% leucine (N-leu 1) at concentrations from 15 to 150 μM, and (d) spray-dried leucine (Leu) at concentrations corresponding to those contained in N-leu 1 (from 0.8 to 7.5 μM). Cell growth was determined using a colorimetric bromodeoxyuridine (BrdU) cell proliferation ELISA kit. The histograms report the percentage of growing cells in comparison with untreated cells (control, 100% proliferation). All data are shown as mean ± SD of three independent experiments each done in duplicate (*$P < 0.05$ and **$P < 0.01$ vs control).
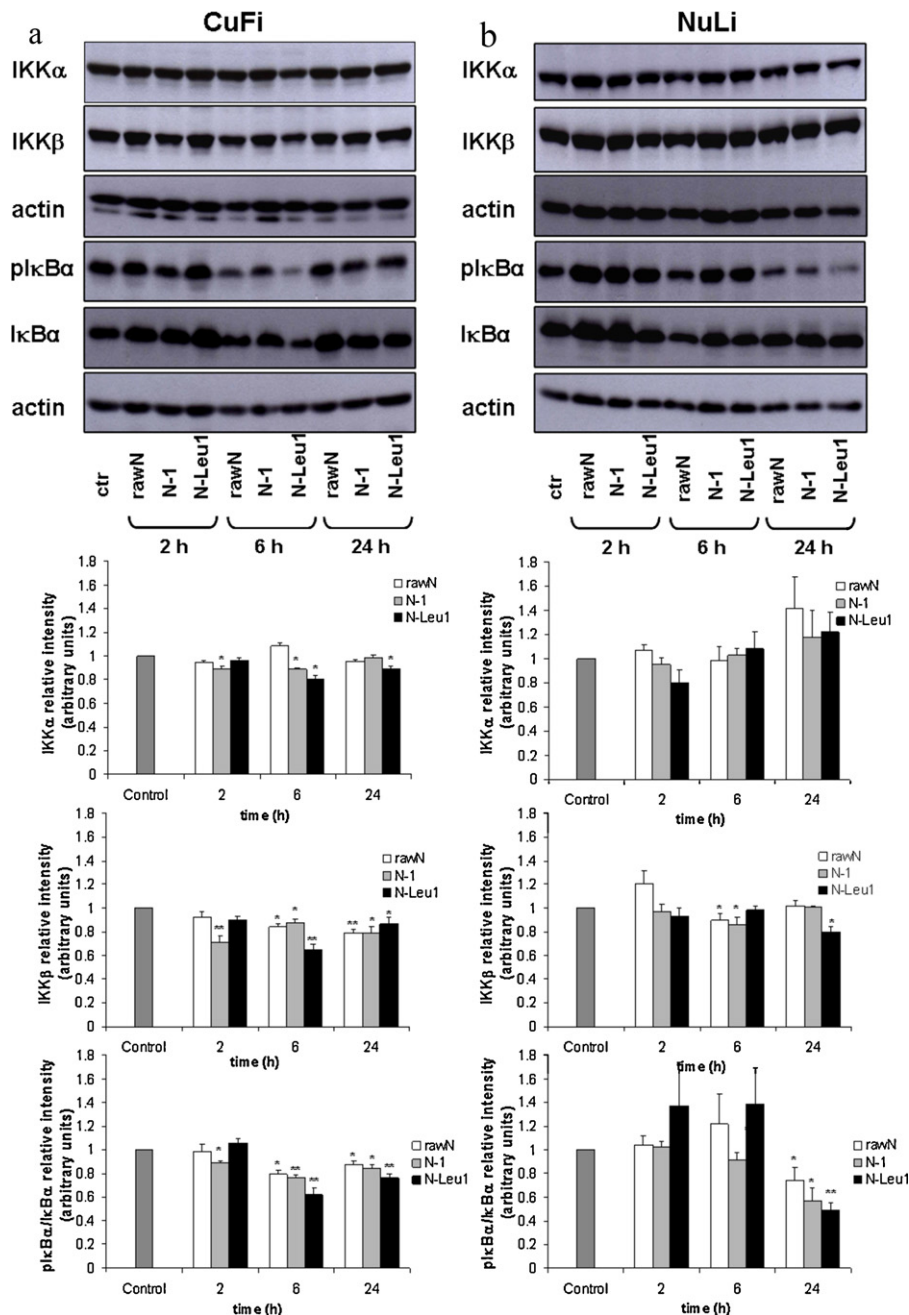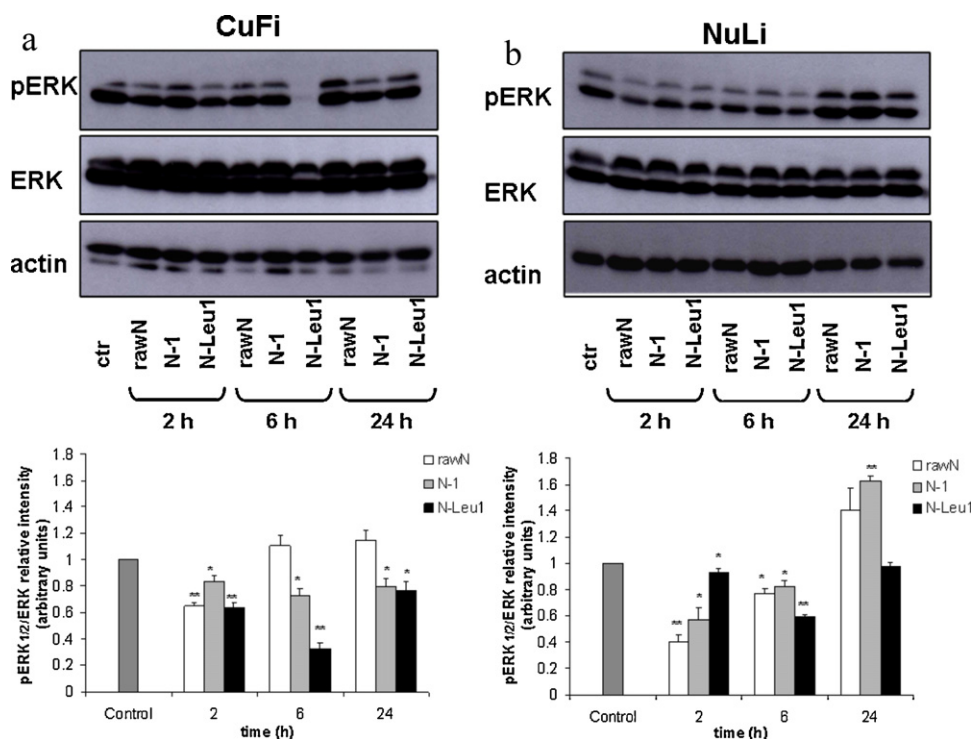
Fig. 9. Naringin and its DPI formulations inhibit the key enzymes of the NF-κB pathway in CF bronchial epithelial cells. CuFi1 (a) and NuLi1 (b) cells were treated with raw Naringin (rawN), spray-dried Naringin (N-1) and N co-sprayed with 5% leucine (N-leu 1) at 30 μM concentration for the indicated time points. Cell lysates were analyzed by Western blot with antibodies against IKKα, IKKβ and pIκBα. Same filters were stripped and re-probed with total IκBα and anti-actin used as loading control. More representative results are shown (upper panels). Immunoreactive bands were quantified using Quantity One program. Densitometric analyses (mean ± SD) of three independent experiments are reported as relative intensity of IKKα, IKKβ or pIκBα/IκBα on actin and expressed as arbitrary units *vs* control (lower panels). (*$P < 0.05$ and **$P < 0.01$ *vs* control).

definitely a prerequisite. As evident from Fig. 7, N-10% AA powders, spray-dried from 50% ethanol feeds had the lowest FPF, corresponding to an undesirable increase of the powders deposition into the throat. N-his 1, N-leu 1 and N-pro 1 showed the best aerodynamic properties in terms of both FPF (about 64%) and FPD (8.47–9.55 mg) and gave satisfactory pulmonary deposition profiles (Fig. 7).

Altogether our data indicate that, when compared to N spray-dried alone, powders processed with 5% AAs from 3:7 ethanol/water and, particularly, N-leu 1 show relatively high improvement of FPF due to both a reduction in the capsule and device retention and/or an increase in the powder dispersibility.

The latter is likely to be related to the absence of aggregates and high degree of particle surface corrugation (Fig. 5). These results are in agreement with previous reports on the ability of surface corrugation to decrease interparticulate cohesion by reducing Van der Waals forces between the particles and, consequently, increase the powder respirability (Chew and Chan, 2001; Chew et al., 2005b).

Another noteworthy finding of our work is the surprisingly high bulk density values of batches N-his 2 and N-leu 3, characterized by almost satisfying FPF (>60%) and FPD (>7.73 mg) (Table 4). From an industrial perspective, high bulk density values imply that the powders are easy to handle and can be introduced in increased

Fig. 10. Naringin and its DPI formulations reduce ERK1/2 phosphorylation in CF airway bronchial epithelial cells. CuFi1 (a) and NuLi1 (b) cells were treated with raw Naringin (rawN), spray dried Naringin (N-1) and N co-sprayed with 5% leucine (N-leu 1) at 30 μM concentration for the indicated time points. Western blot analysis with anti-pERK1/2 (pERK) was performed on cell lysates. Membranes were stripped and re-probed with total ERK1/2 (ERK) and actin as loading control. More representative results are shown (upper panels). Immunoreactive bands were quantified using Quantity One program. Densitometric analyses (mean ± SD) of three independent experiments are reported as relative intensity of pERK/ERK on actin and expressed as arbitrary units *vs* controls (lower panels). (*$P < 0.05$ and **$P < 0.01$ *vs* control).

amounts into the gelatine capsules. Therefore, the ACI deposition experiments were repeated on the capsules containing a double amount (40 mg *vs* 20 mg) of micronized powders. DPIs containing 40 mg of powders were able to emit almost doubled FPDs compared to DPIs charged with 20 mg (Table 4). This result allows to raise the FPD emitted after a single device actuation from about 6.9–8.2 mg (N-1, N-2, N-his 2, and N-leu 3) to 16.2–18.6 mg (N-his 2 bis and N-leu 3 bis), keeping the FPF at about 60%.

3.3. In vitro biological activities of N-dried powders in bronchial epithelial cells

Aim of the research was also to investigate whether N and its formulations could affect intrinsic inflammation of airways epithelium in CF patients. For this scope, we tested rawN, N-1 and N-leu 1 in two immortalized cell lines as *in vitro* models: one, called CuFi1 (CF cells), was derived from human airway epithelial (HAE) cells of CFTR ΔF508/ΔF508 mutant genotype, the other, called NuLi1 (normal lung), was derived from a non-CF subject and used as control. These cell lines exhibited transepithelial resistance, maintained the ion channel physiology expected for the genotypes and retained NF-κB responses to inflammatory stimuli (Dechecchi et al., 2008; Zabner et al., 2003).

Preliminary studies were performed to determine the cytotoxic drug concentration for these cell line models. After a 24 h treatment, rawN did not significantly affect cell viability, as determined by MTT assay in the concentration ranging from 15 to 150 μM (data not shown), but it caused a dose-dependent reduction of cell growth of different extent in NuLi1 and CuFi1 cells, from 60 to 150 μM (Fig. 8a). N-1 did not show a significant effect on proliferation in both cell lines (Fig. 8b), except a slight reduction of cell growth at the highest concentration (150 μM, $P < 0.05$). N-leu 1 induced a dose-dependent and significant cell growth inhibition

only in normal bronchial NuLi1 cells (Fig. 8c), while it determined a 14% increase of cell proliferation in CuFi1 cells at the highest dose (150 μM). In conclusion, neither rawN nor N-1 and N-leu 1 are cytotoxic or cytostatic in both CF and non-CF bronchial epithelial cells at concentrations lower than 60 μM.

To evaluate the contribution of the AA to the increased cell proliferation induced by N-leu 1 in CuFi1, Leu spray-dried alone was also tested. The AA did not show any significant effect in NuLi1 cells while it was able to increase CuFi1 cell proliferation at all the concentrations tested (Fig. 8d). This finding suggests that the technological improvement of immediate drug solubility and powder flowability, as well as the presence of the AA in N-Leu 1, may increase the drug uptake and improve the CF cell altered metabolism, reducing the toxicity observed for unprocessed rawN (Fig. 8a). In accordance, increased and altered basal protein catabolism has been reported in CF patients by many reports (Holt et al., 1985; Levy et al., 1985; Switzer et al., 2009).

To study the anti-inflammatory effects of N in CF cells, we investigated the main molecular targets of NF-κB and MAPK/ERK pathways in CuFi1 in comparison to normal bronchial NuLi1 cells. The NF-κB pathway is well known to play a crucial role in inflammatory process (Yamamoto and Gaynor, 2001). In resting cells, the transcription factor NF-κB exists as homo- or heterodimer, maintained inactive in the cytosol by a family of inhibitor proteins named IκBs (IκBα, β, ε). In response to a wide range of stimuli such as cytokines and bacterial or viral products, IκB proteins are phosphorylated by IκB kinases (IKKα and β), ubiquitinated and degraded by the 26S proteasome. As a consequence, NF-κB dimers can localize into the nucleus and positively regulate the transcription of proinflammatory genes (Hayden and Ghosh, 2004). This pathway is overactivated also in absence of any infection (Lyczak et al., 2002; Rottner et al., 2007; Verhaeghe et al., 2007) in CF cells, as previously reported. In our experiments, CuFi1 cells exhibit higher expression

levels of IKKβ, phosphoIKBα and phosphoERK 1/2 proteins compared to their normal counterpart NuLi1 cells (data from Western Blot analysis not shown). The effects of rawN, N-1 and N-Leu1 at sub-toxic concentrations (30 μM) were evaluated at 2, 6 and 24 h on IKKβ and IκBα kinases, measuring both the expression levels and the phosphorylation status of the main molecular targets of the NF-κB pathway (i.e. IKKα, IKKβ and IκBα). Results are reported in Fig. 9.

As regards to IKKα, N1 and N-leu1 caused a reduction of IKKα but rawN did not in CuFi1 cells, while all powders did not cause any significant effect in NuLi1 cells (Fig. 9b). As IKKβ, its expression was generally reduced in CuFi1 cells: the highest decrease was observed at 6 h in N-leu 1-treated cells (Fig. 9b). In normal bronchial epithelial cells, IKKβ expression was slightly reduced, particularly at 6 h (by N1) and 24 h (by N-leu1). Interestingly, the observed reduction of expression levels of both the enzymatic subunits of the IKK complex in CuFi led to a significant and prolonged decrease of IκBα phoshorylation. In fact, this effect started early (2 h) and was retained all over the treatment time (24 h) in CF bronchial epithelial cells (Fig. 9a). On the contrary, in normal bronchial epithelial cells only a delayed (24 h) decrease of IκBα phosphorylation was observed as a consequence of the reduction of IKKβ subunit only expression level. Leucine spray-dried alone did not give any significant result in all Western Blot analyses (data not shown).

Previous evidence indicates that IKKβ plays a more crucial role for NF-κB activation in response to pro-inflammatory cytokines and microbial products (Verhaeghe et al., 2007), even though both the catalytic subunits of the IKK complex are able to regulate NF-κB activation and have a complementary role in the control of inflammation (Descargues et al., 2008). These observations are in agreement with our results, showing that N formulations are effective in inhibiting both IKK subunits expression, and therefore caused a prolonged reduction of IκBα phosphorylation in CuFi1 cells, whereas the observed slight reduction of IKKβ subunit only may justify the delayed effect on IκBα observed in NuLi1 cells.

As concerns the effect on the MAPK/ERK pathway, results (Fig. 10) showed that N and its formulations, in both NuLi1 and CuFi1 cells, modulate negatively the MAPK/ERK cell signaling pathway, which is known to activate the transcription factor AP-1 required for cytokine transcription and production (Karin, 1995).

However, the effect is very pronounced for N-Leu1 at 6 h and prolonged until 24 h in CF bronchial epithelial cells, with respect to non-CF NuLi1 cells. Also in this case, leucine alone did not induce any change in ERK 1/2 phosphorylation (data not shown). Altogether our findings indicate that N-Leu 1 is able to inhibit both MAPK/ERK and NF-κB pathways, which are over activated in bronchial epithelial cells from CF patients. Furthermore, the evidence collected confirmed the anti-inflammatory properties of flavonoids used in the treatment of chronic vascular and inflammatory diseases (Benavente-Garcia and Castillo, 2008; Manthey et al., 2001).

4. Conclusion

Naringin is a natural polyphenol with anti-inflammatory potential for cystic fibrosis treatment. Particles produced by co-spray drying N and AAs in the appropriate ratio were found to have improved aerodynamic properties, showing high FPFs (>60%), low impact loss, capsule and device retention. The use of leucine as excipient was useful to reduce adhesion between particles and improve powder dispersion when delivered from dry powder inhalers. Therefore, a careful formulation plays a key role in affecting the aerosol performance of N-powders. The formulations were tested in vitro on CF and normal bronchial epithelial cells, to estab-

lish if the particle engineering has positive effect on biological activity.

Since defective CFTR function induces the expression of pro-inflammatory mediators, CF cells show constitutive NF-κB hyperactivation and ERK upregulation, resulting in increased levels of pro-inflammatory mediators also in absence of any infection. N-Leu1 with optimized bulk and aerodynamic behaviour is able to modulate both NF-κB and MAPK/ERK pathways in absence of stimulation in bronchial epithelia, with higher effects in CF cells than in normal bronchial cells.

These findings together with the already reported anti-inflammatory and antioxidant properties of Naringin support a potential use of N/AA-DPI as MAPK and NF-κB inhibitors to treat lung intrinsic inflammation and prevent tissue damages in CF patients.

References

Akabas, M.H., 2000. Cystic fibrosis transmembrane conductance regulator. Structure and function of an epithelial chloride channel. J. Biol. Chem. 275, 3729–3732.

Azbell, C., Zhang, S., Skinner, D., Fortenberry, J., Sorscher, E.J., Woodworth, B.A., 2010. Hesperidin stimulates cystic fibrosis transmembrane conductance regulator-mediated chloride secretion and ciliary beat frequency in sinonasal epithelium. Otolaryngol. Head Neck Surg. 143, 397–404.

Benavente-Garcia, O., Castillo, J., 2008. Update on uses and properties of citrus flavonoids: new findings in anticancer, cardiovascular, and anti-inflammatory activity. J. Agric. Food Chem. 56, 6185–6205.

Chew, N.Y., Chan, H.K., 2001. Use of solid corrugated particles to enhance powder aerosol performance. Pharm. Res. 18, 1570–1577.

Chew, N.Y., Shekunov, B.Y., Tong, H.H., Chow, A.H., Savage, C., Wu, J., Chan, H.K., 2005a. Effect of amino acids on the dispersion of disodium cromoglycate powders. J. Pharm. Sci. 94, 2289–2300.

Chew, N.Y., Tang, P., Chan, H.K., Raper, J.A., 2005b. How much particle surface corrugation is sufficient to improve aerosol performance of powders? Pharm. Res. 22, 148–152.

Chuchalin, A., Amelina, E., Bianco, F., 2009. Tobramycin for inhalation in cystic fibrosis: beyond respiratory improvements. Pulm. Pharmacol. Ther. 22, 526–532.

Dechecchi, M.C., Nicolis, E., Norez, C., Bezzerri, V., Borgatti, M., Mancini, I., Rizzotti, P., Ribeiro, C.M., Gambari, R., Becq, F., Cabrini, G., 2008. Anti-inflammatory effect of miglustat in bronchial epithelial cells. J. Cyst. Fibros. 7, 555–565.

Descargues, P., Sil, A.K., Karin, M., 2008. IKKalpha, a critical regulator of epidermal differentiation and a suppressor of skin cancer. EMBO J. 27, 2639–2647.

Gilani, K., Najafabadi, A.R., Barghi, M., Rafiee-Tehrani, M., 2005. The effect of water to ethanol feed ratio on physical properties and aerosolization behavior of spray dried cromolyn sodium particles. J. Pharm. Sci. 94, 1048–1059.

Giry, K., Pean, J.M., Giraud, L., Marsas, S., Rolland, H., Wuthrich, P., 2006. Drug/lactose co-micronization by jet milling to improve aerosolization properties of a powder for inhalation. Int. J. Pharm. 321, 162–166.

Hancock, B.C., Parks, M., 2000. What is the true solubility advantage for amorphous pharmaceuticals? Pharm. Res. 17, 397–404.

Hayden, M.S., Ghosh, S., 2004. Signaling to NF-kappaB. Genes Dev. 18, 2195–2224.

Heijerman, H., Westerman, E., Conway, S., Touw, D., Doring, G., 2009. Inhaled medication and inhalation devices for lung disease in patients with cystic fibrosis: a European consensus. J Cyst. Fibros. 8, 295–315.

Holt, T.L., Ward, L.C., Francis, P.J., Isles, A., Cooksley, W.G., Shepherd, R.W., 1985. Whole body protein turnover in malnourished cystic fibrosis patients and its relationship to pulmonary disease. Am. J. Clin. Nutr. 41, 1061–1066.

Jacquot, J., Tabary, O., Le Rouzic, P., Clement, A., 2008. Airway epithelial cell inflammatory signalling in cystic fibrosis. Int. J. Biochem. Cell Biol. 40, 1703–1715.

Karin, M., 1995. The regulation of AP-1 activity by mitogen-activated protein kinases. J. Biol. Chem. 270, 16483–16486.

Khan, T.Z., Wagener, J.S., Bost, T., Martinez, J., Accurso, F.J., Riches, D.W., 1995. Early pulmonary inflammation in infants with cystic fibrosis. Am. J. Respir. Crit. Care Med. 151, 1075–1082.

Kieninger, E., Regamey, N., 2010. Targeting inflammation in cystic fibrosis. Respiration 79, 189–190.

Levy, L.D., Durie, P.R., Pencharz, P.B., Corey, M.L., 1985. Effects of long-term nutritional rehabilitation on body composition and clinical status in malnourished children and adolescents with cystic fibrosis. J. Pediatr. 107, 225–230.

Limasset, B., le Doucen, C., Dore, J.C., Ojasoo, T., Damon, M., Crastes de Paulet, A., 1993. Effects of flavonoids on the release of reactive oxygen species by stimulated human neutrophils. Multivariate analysis of structure-activity relationships (SAR). Biochem. Pharmacol. 46, 1257–1271.

Lucas, P., Anderson, K., Potter, U.J., Staniforth, J.N., 1999. Enhancement of small particle size dry powder aerosol formulations using an ultra low density additive. Pharm. Res. 16, 1643–1647.

Lukacs, G.L., Mohamed, A., Kartner, N., Chang, X.B., Riordan, J.R., Grinstein, S., 1994. Conformational maturation of CFTR but not its mutant counterpart (delta F508) occurs in the endoplasmic reticulum and requires ATP. EMBO J. 13, 6076–6086.

Lyczak, J.B., Cannon, C.L., Pier, G.B., 2002. Lung infections associated with cystic fibrosis. Clin. Microbiol. Rev. 15, 194–222.

Manthey, J.A., Grohmann, K., Guthrie, N., 2001. Biological properties of citrus flavonoids pertaining to cancer and inflammation. Curr. Med. Chem. 8, 135–153.

Najafabadi, A.R., Gilani, K., Barghi, M., Rafiee-Tehrani, M., 2004. The effect of vehicle on physical properties and aerosolisation behaviour of disodium cromoglycate microparticles spray dried alone or with L-leucine. Int. J. Pharm. 285, 97–108.

Nicolis, E., Lampronti, I., Dechecchi, M.C., Borgatti, M., Tamanini, A., Bianchi, N., Bezzerri, V., Mancini, I., Giri, M.G., Rizzotti, P., Gambari, R., Cabrini, G., 2008. Pyrogallol, an active compound from the medicinal plant *Emblica officinalis*, regulates expression of pro-inflammatory genes in bronchial epithelial cells. Int. Immunopharmacol. 8, 1672–1680.

Nozaki, Y., Tanford, C., 1971. The solubility of amino acids and two glycine peptides in aqueous ethanol and dioxane solutions. Establishment of a hydrophobicity scale. J. Biol. Chem. 246, 2211–2217.

Parlati, C., Colombo, P., Buttini, F., Young, P.M., Adi, H., Ammit, A.J., Traini, D., 2009. Pulmonary spray dried powders of tobramycin containing sodium stearate to improve aerosolization efficiency. Pharm. Res. 26, 1084–1092.

Peijun, J., Jinxin Zou, Feng, W., 2009. Effect of alcohol on the solubility of amino acid in water. J. Mol. Catal. B: Enzym. 56, 185–188.

Pilcer, G., Amighi, K., 2010. Formulation strategy and use of excipients in pulmonary drug delivery. Int. J. Pharm. 392, 1–19.

Pyle, L.C., Fulton, J.C., Sloane, P.A., Backer, K., Mazur, M., Prasain, J., Barnes, S., Clancy, J.P., Rowe, S.M., 2009. Activation of CFTR by the flavonoid quercetin: potential use as a biomarker of {delta}F508 CFTR rescue. Am. J. Respir. Cell. Mol. Biol..

Ross, K.R., Chmiel, J.F., Konstan, M.W., 2009. The role of inhaled corticosteroids in the management of cystic fibrosis. Paediatr. Drugs 11, 101–113.

Rottner, M., Kunzelmann, C., Mergey, M., Freyssinet, J.M., Martinez, M.C., 2007. Exaggerated apoptosis and NF-kappaB activation in pancreatic and tracheal cystic fibrosis cells. FASEB J. 21, 2939–2948.

Sansone, F., Aquino, R.P., Del Gaudio, P., Colombo, P., Russo, P., 2009. Physical characteristics and aerosol performance of Naringin dry powders for pulmonary delivery prepared by spray-drying. Eur. J. Pharm. Biopharm. 72, 206–213.

Seville, P.C., Li, H.Y., Learoyd, T.P., 2007. Spray-dried powders for pulmonary drug delivery. Crit. Rev. Ther. Drug Carrier Syst. 24, 307–360.

Springsteel, M.F., Galietta, L.J., Ma, T., By, K., Berger, G.O., Yang, H., Dicus, C.W., Choung, W., Quan, C., Shelat, A.A., Guy, R.K., Verkman, A.S., Kurth, M.J., Nantz, M.H., 2003. Benzoflavone activators of the cystic fibrosis transmembrane conductance regulator: towards a pharmacophore model for the nucleotide-binding domain. Bioorg. Med. Chem. 11, 4113–4120.

Switzer, M., Rice, J., Rice, M., Hardin, D.S., 2009. Insulin-like growth factor-I levels predict weight, height and protein catabolism in children and adolescents with cystic fibrosis. J. Pediatr. Endocrinol. Metab. 22, 417–424.

Verhaeghe, C., Remouchamps, C., Hennuy, B., Vanderplasschen, A., Chariot, A., Tabruyn, S.P., Oury, C., Bours, V., 2007. Role of IKK and ERK pathways in intrinsic inflammation of cystic fibrosis airways. Biochem. Pharmacol. 73, 1982–1994.

Virgin, F., Zhang, S., Schuster, D., Azbell, C., Fortenberry, J., Sorscher, E.J., Woodworth, B.A., 2010. The bioflavonoid compound, sinupret, stimulates transepithelial chloride transport in vitro and in vivo. Laryngoscope 120, 1051–1056.

Wegrzyn, G., Jakobkiewicz-Banecka, J., Gabig-Ciminska, M., Piotrowska, E., Narajczyk, M., Kloska, A., Malinowska, M., Dziedzic, D., Golebiewska, I., Moskot, M., Wegrzyn, A., 2010. Genistein: a natural isoflavone with a potential for treatment of genetic diseases. Biochem. Soc. Trans. 38, 695–701.

Yamamoto, Y., Gaynor, R.B., 2001. Role of the NF-kappaB pathway in the pathogenesis of human disease states. Curr. Mol. Med. 1, 287–296.

Zabner, J., Karp, P., Seiler, M., Phillips, S.L., Mitchell, C.J., Saavedra, M., Welsh, M., Klingelhutz, A.J., 2003. Development of cystic fibrosis and noncystic fibrosis airway cell lines. Am. J. Physiol. Lung Cell Mol. Physiol. 284, L844–L854.

Zaman, M.M., Gelrud, A., Junaidi, O., Regan, M.M., Warny, M., Shea, J.C., Kelly, C., O'Sullivan, B.P., Freedman, S.D., 2004. Interleukin 8 secretion from monocytes of subjects heterozygous for the deltaF508 cystic fibrosis transmembrane conductance regulator gene mutation is altered. Clin. Diagn. Lab. Immunol. 11, 819–824.